Chinese Chemical Letters 35 (2024) 109180

Contents lists available at ScienceDirect

Chinese Chemical Letters

journal homepage: www.elsevier.com/locate/cclet

Dual polarization strategy to enhance CH_4 uptake in covalent organic frameworks for coal-bed methane purification

Junhua Wang[b,c], Xin Lian[c], Xichuan Cao[a,b,*], Qiao Zhao[c,**], Baiyan Li[c,**], Xian-He Bu[c]

[a] School of Materials Science and Physics, China University of Mining and Technology, Xuzhou 221116, China
[b] School of Chemical Engineering and Technology, China University of Mining and Technology, Xuzhou 221116, China
[c] School of Materials Science and Engineering, National Institute for Advanced Materials, TKL of Metal and Molecule-Based Material Chemistry, Nankai University, Tianjin 300350, China

ARTICLE INFO

Article history:
Received 2 September 2023
Revised 19 September 2023
Accepted 6 October 2023
Available online 10 October 2023

Keywords:
Dual polarization strategy
Covalent organic frameworks (COFs)
Coal-bed methane purification
Chemical/thermal stability
Cycling stability

ABSTRACT

The purification of low-grade coal-bed methane is extremely important, but challenging, due to the very similar physical properties of CH_4 and N_2. Herein, we proposed a dual polarization strategy by employing triazine and polyfluoride sites to construct polar pores in COF materials, achieving the efficient separation of CH_4 from N_2. As expected, the dual polarized F-CTF-1 and F-CTF-2 exhibit higher CH_4 adsorption capacity and CH_4/N_2 selectivity than CTF-1 and CTF-2, respectively. Especially, the CH_4 uptake capacity and CH_4/N_2 selectivity of F-CTF-2 is 1.76 and 1.42 times than that of CTF-2. This work not only developed promising COF materials for CH_4/N_2 separation, but also provided important guidance for the separation of other adsorbates with similar properties.

© 2024 Published by Elsevier B.V. on behalf of Chinese Chemical Society and Institute of Materia Medica, Chinese Academy of Medical Sciences.

As a kind of unconventional energy with high calorific value, coal-bed methane (CBM) is a kind of natural gas mainly composed of methane and nitrogen [1,2]. For the utilization of coal-bed methane, CBM with the high methane concentration can be directly extracted and utilized [3]. On the contrast, a large number of CBM resources with low methane concentration (<30% CH_4) are often directly vented to the atmosphere, which not only causes resource waste but also aggravates the global greenhouse effect [4–7]. Therefore, the separation of CH_4 from N_2 for low-grade CBM purification is considered to be economical and environment-friendly.

Owing to their similar physical properties, the separation of CH_4/N_2 is widely regarded as one of the most challenging technical issues [8–11]. Currently, traditional industrial technology to separate CH_4 over N_2 from CBM is cryogenic distillation, which is highly energy-consuming and uneconomical [12,13]. On the contrary, adsorbent-based gas separations have exhibited great prospects due to their low energy consumption and simple operation [14]. To date, several types of porous materials have been investigated and used for separating CBM, including activated carbons [15–18], zeolites [19] and MOFs [20–24]. In this regard, activated carbons and zeolites often shows some drawbacks in practical applications including lack of functional adsorption sites, poor separation selectivity, and low uptake capacity [25]. Although MOFs display excellent methane adsorption capacity and CH_4/N_2 separation selectivity because of the existence of unsaturated metal centers and suitable pore size, they often suffer from the poor chemical and moisture stabilities [26–28]. Therefore, it is of great significance to develop highly efficient and stable adsorbents for selective separation of CH_4/N_2.

Covalent organic frameworks (COFs), constructed by covalent bonds, are a type of promising porous materials due to their large specific surface area [29], low mass density [30], excellent chemical/thermal stability [31,32] and structural modularity [33,34]. Therefore, COFs is a kind of suitable candidate material for the separation of CH_4/N_2. Unfortunately, current COFs were rarely reported [35] for methane purification which may be attributed to the lack of efficient constructional strategies. The existing strategy of constructing COF adsorbent for CH_4/N_2 separation is adjusting the pore size of COFs. Therefore, it is necessary to develop new strategy for constructing COF based adsorbents for CH_4/N_2 separation. Based on the fact that CH_4 (25.93×10^{-25} cm^3) has a greater polarizability than N_2 (17.40×10^{-25} cm^3), we reason that enhancing the polarity of the host framework to form multiple interactions between CH_4 molecules and the skeleton would benefit the CH_4/N_2 separation. Therefore, we proposed a dual polar-

* Corresponding author at: School of Materials Science and Physics, China University of Mining and Technology, Xuzhou 221116, China.
** Corresponding authors.
E-mail addresses: xichuancao@cumt.edu.cn (X. Cao), qiaozhao@nankai.edu.cn (Q. Zhao), libaiyan@nankai.edu.cn (B. Li).

https://doi.org/10.1016/j.cclet.2023.109180
1001-8417/© 2024 Published by Elsevier B.V. on behalf of Chinese Chemical Society and Institute of Materia Medica, Chinese Academy of Medical Sciences.

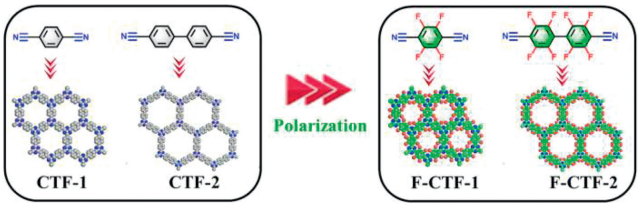

Scheme 1. Illustration of the dual polarization strategy.

ization strategy by introducing both triazine and polyfluoride sites onto framework to construct polar pores, which would thus enhance the interaction between CH_4 molecules and the host framework and thereby achieving the high-efficient separation of CH_4 from N_2.

To verify our strategy, four COFs including CTF-1, CTF-2, and their perfluorinated counterparts (F-CTF-1 and F-CTF-2) were chosen as the platform adsorbents for CBM purification (Scheme 1). Both F-CTF-1 and F-CTF-2 with polar pores exhibited higher CH_4 uptake and CH_4/N_2 selectivity than that of CTF-1 and CTF-2. Especially, F-CTF-2 exhibited high CH_4 uptake capacity (21.7 cm^3/g) and superior CH_4/N_2 selectivity (5.28), which is 1.76 and 1.42 times higher than that of CTF-2. Simulated calculations revealed that the higher CH_4 uptake and CH_4/N_2 selectivity of F-CTF-2 were attributed to the existence of dual polarization sites on COF pores. These results thus highlight the advantage of the dual polarization strategy to construct CH_4 preferred adsorbent for CH_4/N_2 separation. Additionally, F-CTF-2 exhibits excellent chemical and thermal stabilities, making it among the promising adsorbents for CBM purification.

All of the COF materials were prepared at 500 °C under typical ionothermal conditions using $ZnCl_2$ as catalyst with a $ZnCl_2$/monomer molar ratio of 10 [36]. The obtained products were abbreviated as CTF-1, CTF-2, F-CTF-1, F-CTF-2, respectively. The successful synthesis of CTFs and F-CTFs was confirmed by Fourier transform-infrared (FT-IR), X-ray photoelectron spectroscopy (XPS), solid-state ^{13}C NMR measurements. As shown in the FT-IR spectra (Fig. 1a and Fig. S1 in Supporting information), the characteristic vibrational band for the terminal cyano group at ~2248 cm^{-1} disappeared after polymerization, representing the complete polymerization has been achieved. Meanwhile, the new characteristic vibrations at ~1569 cm^{-1} (–C=N– stretching vibration) and 1373 cm^{-1} (–C–N= stretching vibration) indicated the successful formation of the triazine rings [36,37]. Furthermore, X-ray photoelectron spectroscopy (XPS) was used to verify the structural features of the CTFs and F-CTFs. As displayed in Figs. S2a and b (Supporting information), the C 1s XPS spectrum of each of the samples can be resolved into two peaks. The strongest peak (284.9 eV) was assigned to the sp^2 hybrid C species in the benzene rings, while the peak with higher binding energy (286.2 eV) was assigned to the sp^2 hybrid C species in the triazine rings [38]. In the N 1s XPS spectra of CTFs and F-CTFs, the peaks at ~398.0 eV also revealed the formation of the triazine rings (Fig. 1b and Fig. S2c in Supporting information) [39]. Solid-state ^{13}C NMR spectra of F-CTFs showed the characteristic peak at ~161 ppm corresponding to the sp^2-hybridized carbon atoms in the triazine ring [40], which further revealed the formation of CTFs (Fig. S3 in Supporting information). Additionally, the morphology of F-CTFs was analyzed by the SEM and TEM. The layered structures and porosity were observed. The energy dispersive spectroscopy (EDS) elemental mappings (Fig. S4 in Supporting information) indicated a homogeneous distribution of C, N and F in F-CTFs. Finally, the powder X-ray diffraction (XRD) patterns of CTFs and F-CTFs showed an amorphous character (Fig. S5 in Supporting information).

The porosity property of the model COF materials was examined by N_2 adsorption isotherms at 77 K (Fig. 2a). All of the samples displayed rapid N_2 uptake at low relative pressures ($P/P_0 < 0.04$), indicating the existence of microporous structures. Then, the hysteresis loops appeared around the relative pressure of $P/P_0 = 0.4$, showing the presence of mesopores. The formation of mesoporous structure may be caused by the defects in CTFs [41]. The Brunauer-Emmett-Teller (BET) specific surface areas of CTF-1 and CTF-2 were calculated to be 1239 and 1599 m^2/g. And that were 1392 and 1812 m^2/g for F-CTF-1 and F-CTF-2, respectively. In addition, the pore size distributions were calculated by the density

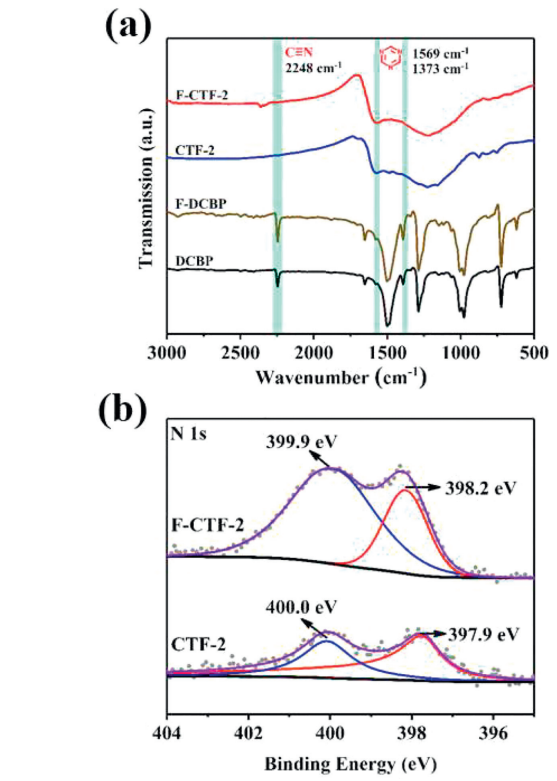

Fig. 1. (a) FT-IR, (b) N 1s XPS spectra of CTF-2 and F-CTF-2.

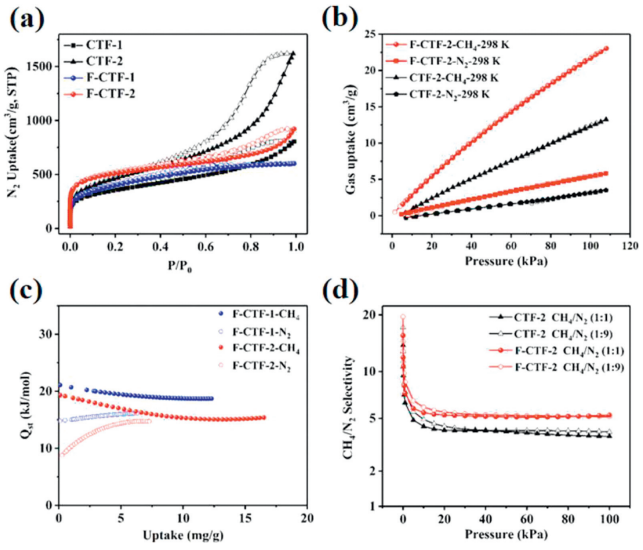

Fig. 2. (a) Nitrogen sorption isotherms at 77 K. (b) Single-component adsorption isotherms of CH_4 and N_2 for CTF-2 and F-CTF-2 at 298 K. (c) Q_{st} curves for F-CTF-1 and F-CTF-2. (d) IAST selectivity of CH_4/N_2 (1:1, v/v and 1:9, v/v) for CTF-2 and F-CTF-2 at 298 K.

functional theory model (Fig. S6 in Supporting information). Compared with CTF-1 and CTF-2, F-CTF-1 and F-CTF-2 possessed more ultramicropore structures at 5.9 Å and 5.0 Å, which favors small-size gas molecule separation.

In order to verify the effectiveness of the dual polarization strategy, the single-component adsorption of CH_4 and N_2 was separately measured at 273 and 298 K (Fig. 2b, Figs. S7a and b in Supporting information). The adsorption capacities of F-CTF-1 and F-CTF-2 for CH_4 at 273 K and 1 bar were 25.2 cm^3/g and 33.7 cm^3/g, respectively. While the CH_4 uptake for CTF-1 and CTF-2 were a little lower with the capacity of 23.3 cm^3/g and 20.2 cm^3/g, respectively, under the identical conditions. Consistently, the CH_4 uptake of F-CTF-1 and F-CTF-2 at 298 K and 1 bar were also higher than their counterparts of CTF-1 (16.3 *vs.* 14.9 cm^3/g) and CTF-2 (21.7 *vs.* 12.3cm^3/g), respectively. Apparently, all F-CTFs absorbed more CH_4 than their non-fluorizated counterparts in the full pressure region at 298 K or 273 K. Then, the virial equation was used to calculate isosteric enthalpy of adsorption (Q_{st}) for all samples based on the isotherms collected at 273 K and 298 K (Fig. 2c and Fig. S7c in Supporting information). The fitted parameters were provided in Tables S1–S4 (Supporting information). The initial Q_{st} values of CH_4 for F-CTF-1 and F-CTF-2 were 21.1 and 19.4 kJ/mol, respectively, higher than those for CTF-1 and CTF-2 (17.6 and 16.7 kJ/mol, respectively). As descripted, both the CH_4 uptake and Q_{st} follow the trend: CTFs<F-CTFs. This phenomenon is due to the introduction of polar sites on F-CTFs pores, which induce a stronger guest-framework interaction. To explore the separation potential of adsorbents, the CH_4/N_2 separation abilities of these COFs were evaluated by the ideal adsorbed solution theory (IAST) calculations (Tables S5 and S6 in Supporting information). Consistent with the trend of CH_4 uptake for CTFs and F-CTFs, the adsorption selectivities of the CH_4/N_2 (1:1, v/v) mixture at 298 K and 1 bar for F-CTF-1 and F-CTF-2 were 5.20 and 5.28, respectively (Fig. 2d and Fig. S7d in Supporting information), higher than that of CTF-1 (4.59) and CTF-2 (3.73). Notably, the selectivity of F-CTFs are higher than that of many benchmark adsorbents, such as 5A zeolite (1.7) [42], BPL (2.6) [43] and MIL-100(Cr) (3.0) [44], indicating the successful practice of dual polarization strategy.

Considering the practical application, the stability of adsorbent is another key criterion to evaluate the industrial application potential for the purification of CBM. As an optimized candidate, the chemical/thermal stabilities for F-CTF-2 were investigated. F-CTF-2 can remain structurally stable in harsh conditions as verified by the consistent FT-IR results (Fig. S8a in Supporting information) and almost the same CH_4 uptake capacity after being treated in 6 mol/L HCl and 6 mol/L NaOH solution for 72 h, respectively (Fig. S8b in Supporting information). TGA test showed that F-CTF-2 possessed a high thermal stability up to 450 °C (Fig. S9 in Supporting information). Moreover, F-CTF-2 exhibited superior recyclability with no visible decay after 10 cycles (Fig. S10 in Supporting information). It is worth noting that the comprehensive applicability of F-CTF-2 has exceeded that of most other benchmarks, such as zeolites [19], MOFs [1], Schiff-based COFs [45], which often suffer from the potential decomposition of porous structures under such harsh conditions (Fig. 3) [46,47]. Therefore, these results thus rank F-CTF-2 among the best porous adsorbents for CBM purification.

The adsorption behavior of CH_4 and N_2 was computed using grand canonical Monte Carlo simulations to reveal the adsorption mechanism. Considering its superior CH_4 adsorption capacity and CH_4/N_2 selectivity, F-CTF-2 was chosen as the simulation model. As illustrated in Fig. 4a, CH_4 interacted with the fluorine binding sites of F-CTF-2 *via* multiple C–H···F hydrogen bond interactions, in which the H···F distance ranged from 2.98 Å to 4.08 Å. Meanwhile, CH_4 interacted with the triazine ring sites *via* multiple C–H···N hydrogen bond interactions, and the H···N distance differed from 3.83 Å to 4.41 Å. In comparison, there only existed weak Van

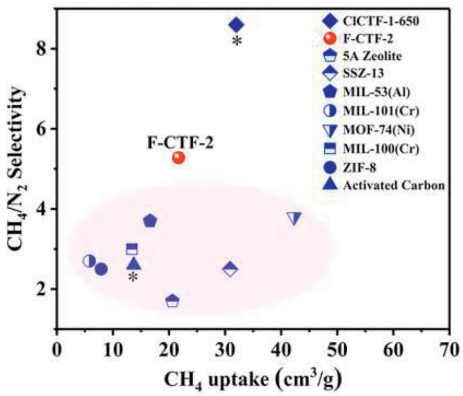

Fig. 3. Comparison of separation performance on F-CTF-2 and other benchmarks (*chemical stability was not studied).

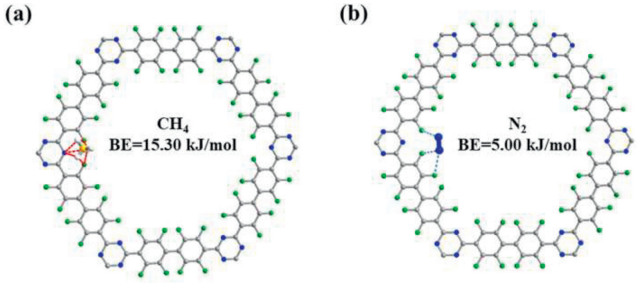

Fig. 4. Schematic adsorption sites for (a) CH_4 and (b) N_2 obtained from theoretical calculations. Color code: C, dark gray; H, white; N, blue; F, green.

der Waals interactions between N_2 and the F-CTF-2 host frameworks with the N···F distance from 4.14 Å to 4.58 Å (Fig. 4b). This is consistent with the calculated binding energy of 15.30 kJ/mol between F-CTF-2 and CH_4, and a low binding energy of 5.00 kJ/mol between F-CTF-2 and N_2. The stronger interactions between the dual polarization sites in skeleton and methane molecules could thus account for high methane uptake and selectivity for F-CTF-2.

To further confirm the practical separation performance on the CBM with a low CH_4 concentration, breakthrough experiment of F-CTF-2 for CH_4/N_2 (1:9, v/v) was purged into a packed column with a total inlet flow rate of 10 mL/min at 298 K (Fig. 5). During the experiment, N_2 firstly penetrated the column before CH_4 because of weaker interactions with the adsorbents. Subsequently, CH_4 broke through the column after 20 min, which corresponds to a time window of 20 min for high-purity CH_4 collection. This separation experiment demonstrated that F-CTF-2 can efficiently purify

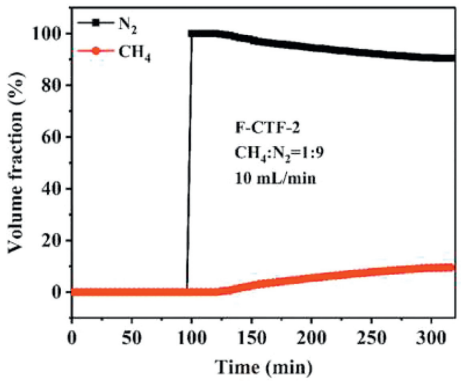

Fig. 5. Experimental breakthrough curve for F-CTF-2 at 298 K and 1 bar.

low concentration CBM, indicating the practicability of the dual polarization strategy.

In conclusion, we developed a dual polarization strategy to construct robust adsorbents for coal-bed methane purification. By introducing triazine and polyfluoride sites onto COF-based materials, the CH_4 uptake and CH_4/N_2 selectivity were significantly enhanced. This was attributed to the enhanced affinity between CH_4 molecules and the skeleton. Theoretical calculation revealed that the surface of F-CTF-2 could have strong interactions with CH_4 *via* multiple C-H···F and C-H···N hydrogen bonds, which then caused good CH_4 adsorption capacity. Thereby our work not only proposed a new approach to prepare high uptake CH_4 adsorbents but also provided insight of the development of COFs as a new type of adsorbents for low concentration coal-bed methane purification.

Declaration of competing interest

The authors declare that they have no known competing financial interests or personal relationships that could have appeared to influence the work reported in this paper.

Acknowledgments

This work was supported by National Key R&D Program of China (No. 2022YFA1503300), National Natural Science Foundation of China (Nos. 21978138, 22035003), the Fundamental Research Funds for the Central Universities (Nankai University), and the Haihe Laboratory of Sustainable Chemical Transformations (No. YYJC202101).

Supplementary materials

Supplementary material associated with this article can be found, in the online version, at doi:10.1016/j.cclet.2023.109180.

References

[1] S.M. Wang, M. Shivanna, Q.Y. Yang, Angew. Chem. Int. Ed. 61 (2022) e202201017.
[2] T.Y. Li, Y.S. Wang, M.Y. Zhang, et al., Chem. Eng. J. 462 (2023) 142118.
[3] Y. Liu, Q. Xu, L. Chen, et al., Nano Res. 15 (2022) 7695–7702.
[4] C. Zhang, Y. Chen, H. Wu, et al., Chem. Eng. J. 435 (2022) 133876.
[5] Q. Shi, J. Wang, H. Shang, et al., Sep. Purif. Technol. 230 (2020) 115850.
[6] M. Chang, F. Wang, Y. Wei, et al., AIChE J. 68 (2022) e17794.
[7] J. Liu, X. Tang, X. Liang, et al., AIChE J. 68 (2022) e17589.
[8] F. Zhang, H. Shang, B. Zhai, et al., AIChE J. 69 (2023) e18079.
[9] M. Chang, T. Yan, Y. Wei, et al., ACS Appl. Mater. Interfaces 14 (2022) 25374–25384.
[10] X.W. Liu, Y.M. Gu, T.J. Sun, et al., Ind. Eng. Chem. Res. 58 (2019) 20392–20400.
[11] M. Chang, J. Ren, Y. Wei, et al., Chem. Mater. 35 (2023) 4286–4296.
[12] D. Lv, Y. Wu, J. Chen, et al., AIChE J. 66 (2020) e16287.
[13] V.I. Águeda Maté, J.A. Delgado Dobladez, S. Álvarez-Torrellas, et al., Chem. Eng. J. 361 (2019) 1007–1018.
[14] M. Chang, Y. Zhao, D. Liu, et al., Sustain. Energy Fuels 4 (2020) 138–142.
[15] S. Xu, W.C. Li, C.T. Wang, et al., Angew. Chem. Int. Ed. 60 (2021) 6339–6343.
[16] P. Zhang, J. Wang, W. Fan, et al., Chem. Eng. J. 375 (2019) 121931.
[17] Z. Dong, B. Li, H. Shang, et al., AIChE J. 67 (2021) e17281.
[18] S.M. Wang, P.C. Wu, J.W. Fu, Q.Y. Yang, Sep. Purif. Technol. 274 (2021) 119121.
[19] X. Tang, Y. Wang, M. Wei, et al., Sep. Purif. Technol. 318 (2023) 124003.
[20] Z. Niu, X. Cui, T. Pham, et al., Angew. Chem. Int. Ed. 58 (2019) 10138–10141.
[21] S. Qadir, D. Li, Y. Gu, et al., Chem. Eng. J. 408 (2021) 127238.
[22] M. Chang, J. Ren, Q. Yang, D. Liu, Chem. Eng. J. 408 (2021) 127294.
[23] Y. Chen, Y. Wang, Y. Wang, et al., AIChE J. 68 (2022) e17819.
[24] D. Lv, R. Shi, Y. Chen, et al., Ind. Eng. Chem. Res. 57 (2018) 12215–12224.
[25] Y. Chen, H. Wu, Y. Yuan, et al., Chem. Eng. J. 385 (2020) 123836.
[26] T. Li, X. Jia, H. Chen, et al., ACS Appl. Mater. Interfaces 14 (2022) 15830–15839.
[27] X. Zhao, P. Pachfule, A. Thomas, Chem. Soc. Rev. 50 (2021) 6871–6913.
[28] J.N. Chang, Q. Li, Y. Yan, et al., Angew. Chem. Int. Ed. 61 (2022) e202209289.
[29] X.H. Han, J.Q. Chu, W.Z. Wang, et al., Chin. Chem. Lett. 33 (2022) 2464–2468.
[30] X. Feng, X. Ding, D. Jiang, Chem. Soc. Rev. 41 (2012) 6010–6022.
[31] J. Li, J. Wang, F. Shui, et al., Chin. Chem. Lett. 34 (2023) 107917.
[32] J.N. Chang, Q. Li, J.W. Shi, et al., Angew. Chem. Int. Ed. 62 (2023) e202218868.
[33] T.Y. Yu, Q. Niu, Y. Chen, et al., J. Am. Chem. Soc. 145 (2023) 8860–8870.
[34] M.X. Wu, Y.W. Yang, Chin. Chem. Lett. 28 (2017) 1135–1143.
[35] K.X. Yao, Y. Chen, Y. Lu, Y. Zhao, Y. Ding, Carbon 122 (2017) 258–265.
[36] P. Kuhn, M. Antonietti, A. Thomas, Angew. Chem. Int. Ed. 47 (2008) 3450–3453.
[37] X. Suo, F. Zhang, Z. Yang, et al., Angew. Chem. Int. Ed. 60 (2021) 25688–25694.
[38] G. Wang, K. Leus, H.S. Jena, et al., J. Mater. Chem. A 6 (2018) 6370–6375.
[39] Z.A. Lan, M. Wu, Z. Fang, et al., Angew. Chem. Int. Ed. 61 (2022) e202201482.
[40] X. Zhu, C. Tian, S.M. Mahurin, et al., J. Am. Chem. Soc. 134 (2012) 10478–10484.
[41] M. Liu, Q. Huang, S. Wang, Angew. Chem. Int. Ed. 57 (2018) 11968–11972.
[42] J.A.C. Silva, A. Ferreira, P.A.P. Mendes, et al., Ind. Eng. Chem. Res. 54 (2015) 6390–6399.
[43] S. Sircar, J. Chem. Soc. Faraday Trans. I 80 (1984) 1101–1111.
[44] L. Li, J. Yang, J. Li, Y. Chen, J. Li, Microporous Mesoporous Mater. 198 (2014) 236–246.
[45] L. Liao, X. Guan, H. Zheng, et al., Chem. Sci. 13 (2022) 9305–9309.
[46] A. Dong, D. Chen, Q. Li, et al., Small 19 (2023) 2201550.
[47] X. Guan, H. Li, Y. Ma, et al., Nat. Chem. 11 (2019) 587–594.